Ab Initio Quantum Chemical Studies of the Formaldiminoxy (CH_2NO) Radical: 1. Isomerization Reactions

Warwick A. Shapley and George B. Bacskay*

School of Chemistry, University of Sydney, NSW 2006, Australia

Received: December 30, 1998; In Final Form: April 5, 1999

A detailed ab initio quantum chemical investigation of the potential energy surface associated with the isomerization reactions of the formaldiminoxy (CH_2NO) radical is reported. $CH_2NO(^2A')$ is the direct product of the reaction between triplet methylene and "prompt" nitric oxide. The quantum chemical calculations were performed at the Gaussian-2 (G2), CASSCF, CASPT2, and QCISD(T) levels of theory using basis sets that range from cc-pVDZ and cc-pVTZ up to the 6-311+G(3df,2p) of G2. A total of 11 isomers (plus 9 rotamers) and 28 transition states linking them are identified and characterized on the potential energy surfaces. The isomers and their rearrangement reactions are conveniently divided into two classes: those with CNO- and NCO-chain backbones. The latter class of molecules are generally more stable, with the NH_2CO isomer being the most stable with a predicted heat of formation of -3.6 ± 1 kcal/mol. Interconversion between the two groups occurs via a cyclic isomer of CH_2NO. The energetics of the various isomerization pathways are expected to influence the subsequent dissociation reactions of the formaldiminoxy isomers.

Introduction

In addition to its formation from fuel-bound nitrogen, nitric oxide (NO) may also be formed in combustion systems by the direct or indirect oxidation of atmospheric nitrogen.[1] Direct oxidation proceeds by the "thermal" mechanism and involves reaction of N_2 with O atoms whereas indirect oxidation initially involves the reaction of N_2 with small hydrocarbon radicals such as CH and CH_2. The compounds so formed subsequently react to form the so-called "prompt" NO.[2] These same hydrocarbon radicals also react with the NO generated, a process referred to as "reburning",[3−6] and thus play a part in *decreasing* the amount of NO emitted. The formaldiminoxy radical, CH_2NO, is an important intermediate generated in the reburning of nitric oxide by methylene during combustion processes. The direct experimental studies on this system have focused largely on the measurement of the rate constant[7−10] of the reaction

$$CH_2 + NO \rightarrow \text{products} \qquad (1)$$

as well as the spectroscopic characterization of CH_2NO itself.[10−13]

In a previous study[14] we have reported the results of our ab initio studies of the association reaction between CH_2 and NO and of a number of the subsequent isomerization and decomposition reactions of CH_2NO. Specifically, we found that two isomers CH_2NO and CH_2ON can form and interconvert by a unimolecular process via a cyclic intermediate. CH_2NO is, however, the more stable of the two and is formed by a barrierless combination of CH_2 and NO. CH_2ON, on the other hand, experiences a small barrier to its formation and as it is thermodynamically unstable (a characteristic shared by other isomers with C−O−N backbones), it readily isomerizes to CH_2-NO. The loss of H and H_2 from CH_2NO was also examined and found to be energetically feasible, although the most viable mechanism for the production of H_2 + CNO was found to be abstraction by H. The calculations were performed using the Gaussian-2 (G2) method[15] which is believed to have yielded chemically accurate energies for equilibrium structures and, in the main, for transition states as well. In some instances, however, as a result of incorrect MP2 bond lengths, G2 gave erroneous energies for transition states that are associated with bond dissociation or abstraction reactions. By way of comparison, CASSCF[16,17] geometries and frequencies were also computed, as well as highly correlated electronic energies obtained by QCISD(T),[18] CCSD(T),[19] and CASPT2[20,21] computations using larger basis sets.

The association reaction between triplet CH_2 and NO and several of the decomposition reactions of the resulting formaldiminoxy radical have also been the subject of a recent study by Roggenbuck and Temps.[22] Using density functional as well as the G2 method, these workers have elucidated the pathways leading to the formation of two cyclic and two open-chain isomers of CH_2NO as well as the decomposition channels to HCN + OH, H + HCNO, and H_2 + CNO.

In this paper, we present further results of our quantum chemical studies on the CH_2NO system which include a comprehensive study of the potential energy surfaces associated with all but the most improbable (high energy) isomerization pathways. Eleven distinct isomers and 24 transition states are considered as well as several rotamers of these. For the sake of completeness these include the five isomers and six transition states described by Roggenbuck and Temps.[22] The dissociation reactions of the isomers considered in this work form the subject of our next paper on the formaldiminoxy system.[23] The purpose of these studies has been the elucidation of the energetics and mechanisms of the reactions of this interesting system with a view to providing data that could be used in subsequent kinetic modeling studies. Although many experimental and theoretical studies have been undertaken to examine the role of the various elementary reactions associated with the production and elimination of nitric oxides (NO_x) during combustion, to the best of our knowledge no detailed experimental study of the isomerizations of the CH_2NO radical has yet been made.

* Corresponding author.

10.1021/jp984817e CCC: $18.00
Published on Web 05/22/1999

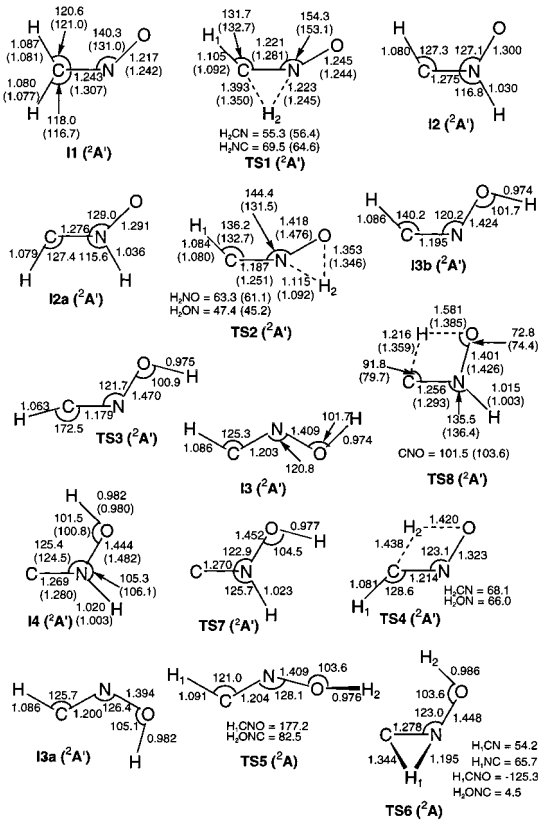

Figure 1. MP2/6-31G(d) geometries and CASSCF(11/11)/cc-pVDZ geometries (in parentheses) of species corresponding to stationary points on the PES describing the CNO chain isomerizations (in Å and deg).

Computational Methods

The bulk of the computational work has been performed using the Gaussian-2 (G2) method,[15] whereby the geometries and harmonic frequencies of all species of interest are calculated as well as their energies. Given the high levels of theory which are employed in a composite G2 calculation of electronic energies, heats of reactions are generally predicted within about 2 kcal/mol of experimentally determined values. A similar level of accuracy may be demonstrated in the computation of critical energies, provided of course that a single-reference-based treatment, which is implicit in G2, is applicable. By way of comparison and also as a check of the G2 results, the geometries and frequencies of a number of species, particularly those of transition states, have also been computed by the CASSCF method[16,17] using Dunning's cc-pVDZ basis,[24] followed by (single point) computation of their electronic energies utilizing the CASPT2[20,21] as well as QCISD(T)[18] techniques, in conjunction with the cc-pVTZ basis set.[24] As in our previous work,[14] the CASSCF frequencies were scaled by the factor 0.92. Such scaling was found to result in reasonable agreement between the CASSCF and the analogous SCF/6-31G(d) frequencies used in the G2 approach.[25] The choice of active space, viz. 11 electrons in 11 active orbitals, was also arrived at on the basis of our previous studies, finding it reliable with regard to the computation of transition state geometries and energies. For molecules with C_s symmetry, the active space consists of seven and four orbitals of a′ and a″ symmetry, respectively. The QCI method, employing unrestricted Hartree−Fock (UHF) wave functions as reference states, has the capacity to yield accurate energies, even in the presence of considerable near-degeneracy that would make Møller−Plesset perturbation theory inapplicable. QCI can thus provide a useful alternative to CASPT2.

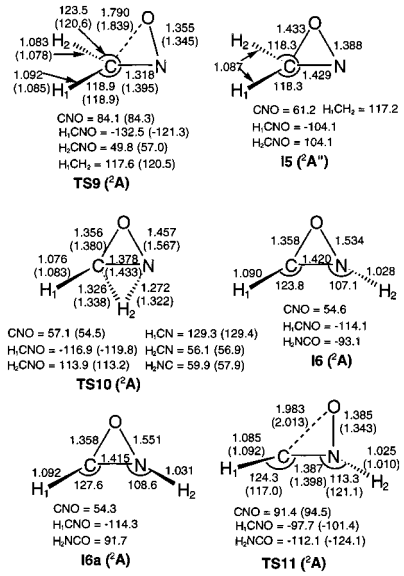

Figure 2. MP2/6-31G(d) geometries and CASSCF(11/11)/cc-pVDZ geometries (in parentheses) of species corresponding to stationary points on the PES describing the isomerizations of the ring structures (in Å and deg).

The computations were performed using the Gaussian 94,[26] Dalton,[27] and MOLCAS4[28] codes on DEC alpha 600/5/333 workstations.

Results and Discussion

As we have discussed in our previous paper,[14] the association of methylene and nitric oxide to give the formaldiminoxy radical (CH_2NO) is exothermic by about 76.5 kcal/mol. Provided no thermal equilibration takes place, this energy could be used to facilitate subsequent isomerization and dissociation. Alternatively, what reactions CH_2NO will undergo depends on the experimental conditions, viz., temperature and pressure.

In the study of the isomerization reactions the systems are subdivided into three classes on the basis of their structures, which are molecules with CNO, NCO, or CON chains respectively as the molecular "backbones", with cyclic systems providing the connections between them. As will be shown, the NCO-chain isomers are generally the most stable, followed by the CNO-chain molecules, with the CON-chain molecules being least stable. This last group includes only three isomers: H_2CON, HCONH, and H_2NOC, i.e., a nitrene, carbene, and carbyne, respectively. The formation and decomposition of the most stable of these molecules (H_2CON) has been discussed in our previous paper. Our attempts to find equilibrium geometries for the high-spin quartet and low-spin doublet states of H_2NOC resulted in weakly bound $NH_2O + C$ and $NH_2 + CO$ systems, respectively, rather than stable isomers of CH_2NO. Given that the remaining isomer, HCONH, is quite energetic, with a G2 energy that is 70.8 kcal/mol above CH_2NO, it is not expected to make important contributions to the overall isomerization and decomposition reactions and therefore it is not included in the current study.

CNO-Chain and Ring Isomers. The MP2/6-31G(d) and CASSCF(11/11)/cc-pVDZ geometries of stationary points corresponding to isomers and transition states involving linear and ring CNO structures are shown in Figures 1 and 2. The associated G2, CASPT2, and QCISD(T) electronic and G2 and CASSCF zero-point vibrational energies are listed in Tables 1 and 2. Four stable CNO-chain isomers have been found on the

TABLE 1: G2 Total and Zero-Point Vibrational Energies of Isomers and Transition States Associated with the Isomerization Reactions of CH_2NO[a]

	G2[b] (E_h)	ΔE_{ZPE}(G2) (kcal/mol)		G2[b] (E_h)	ΔE_{ZPE}(G2) (kcal/mol)
$CH_2NO(^2A')$ (I1)	−168.930 826	18.43	HNC(H)O(^{2}A) (I7)	−168.962 679	18.90
$CH_2NO(^2A'')$ (I1a)	−168.900 925[c]	18.16[c]	HNC(H)O($^2A'$) (I7a)	−168.949 556	19.90
TS1($^2A'$)	−168.809 506	15.29	HNC(H)O($^2A'$) (I7b)	−168.945 673	19.88
TS1a($^2A''$)	−168.775 123[d]	14.17[d]	SC13($^2A''/^2A''$)	−168.837 696[e]	16.33[e]
HCN(H)O($^2A'$) (I2)	−168.860 460	18.68	$NCH_2O(^2A')$ (I8)	−168.840 316	18.27
HCN(H)O($^2A'$) (I2a)	−168.855 981	18.46	TS14(^{2}A)	−168.841 779	15.12
HCN(H)O($^2A''$) (I2b)	−168.846 816	19.64	TS15(^{2}A)	−168.915 317	15.98
TS2($^2A'$)	−168.807 742[e]	15.13[e]	TS15a(^{2}A)	−168.912 646	15.58
HCNOH($^2A'$) (I3b)	−168.891 386	18.31	$NH_2CO(^2A')$ (I9)	−168.996 242	19.90
TS3($^2A'$)	−168.885 315[e]	17.45[e]	$NH_2CO(^2A'')$ (I9a)	−168.882 342	19.64
HCNOH($^2A'$) (I3)	−168.896 529	18.58	TS16($^2A''$)	−168.965 042[e]	17.88[e]
HCNOH($^2A''$) (I3c)	−168.815 615	18.39	TS16a($^2A''$)	−168.961 452[e]	17.63[e]
TS4($^2A'$)	−168.802 906	14.67	TS16b($^2A'$)	−168.946 084	18.45
HCNOH($^2A'$) (I3a)	−168.892 216	18.47	TS17($^2A'$)	−168.899 378	16.66
TS5(^{2}A)	−168.886 946	17.76	HNCOH($^2A'$) (I10a)	−168.963 629	19.71
TS6(^{2}A)	−168.812 729	15.59	TS18(^{2}A)	−168.956 381	19.03
CN(H)OH($^2A'$) (I4)	−168.864 042	19.03	HNCOH($^2A'$) (I10)	−168.964 595	19.59
TS7($^2A'$)	−168.854 948	18.73	TS19($^2A'$)	−168.909 697	15.89
TS8($^2A'$)	−168.822 934	16.12	TS20(^{2}A)	−168.835 096	15.28
TS9(^{2}A)	−168.865 014	16.16	NC(H)OH($^2A'$) (I11)	−168.968 959	19.60
cyclic $CH_2NO(^2A'')$ (I5)	−168.907 165	19.77	TS21(^{2}A)	−168.958 686	18.49
TS10(^{2}A)	−168.807 352	15.70	NC(H)OH($^2A'$) (I11a)	−168.964 100	19.22
cyclic C(H)N(H)O(^{2}A) (I6)	−168.870 180	19.87	TS22(^{2}A)	−168.902 953	16.17
cyclic C(H)N(H)O(^{2}A) (I6a)	−168.868 277	19.80	TS23($^2A'$)	−168.912 217	16.09
TS11(^{2}A)	−168.788 055	17.88	TS24(^{2}A)	−168.901 807	16.00
TS12(^{2}A)	−168.858 249	18.42			

[a] At MP2/6-31G(d) geometry. [b] G2 energy includes the zero-point correction ΔE_{ZPE}(G2). [c] Possesses an imaginary a″ frequency. [d] Second-order saddle point. [e] Using scaled MP2 frequencies.

TABLE 2: CASPT2 and QCISD(T) Total and Zero-Point Vibrational Energies of Selected Isomers and Transition States Associated with the Isomerization Reactions of CH_2NO[a]

	CASPT2(11/11) cc-pVTZ (E_h)	QCISD(T) cc-pVTZ (E_h)	ΔE_{ZPE}-(CASSCF(11/11)) (kcal/mol)
$CH_2NO(^2A')$ (I1)	−168.928 014	−168.919 733	18.87
	−168.926 279[b]	−168.918 019[b]	
TS1($^2A'$)	−168.794 531	−168.793 029	13.96
TS2($^2A'$)	−168.792 585	−168.786 467	14.40
TS8($^2A'$)	−168.802 065	−168.800 985	15.90
	−168.815 036[b]	−168.807 654[b]	
TS9(^{2}A)	−168.860 126	−168.849 921	17.67
CN(H)OH($^2A'$) (I4)	−168.853 227	−168.853 623	18.07
cyclic $CH_2NO(^2A'')$ (I5)	−168.900 394	−168.896 980	19.05
TS10(^{2}A)	−168.795 194	−168.790 832	15.05
TS11(^{2}A)	−168.795 153	−168.781 788	16.93
	−168.793 896[b]	−168.778 844[b]	
TS12(^{2}A)	−168.853 492	−168.850 524	17.57

[a] At CASSCF(11/11)/cc-pVDZ geometry unless stated otherwise. [b] At MP2/6-31G(d) geometry.

molecular potential energy surface. In order of energy they are

$$CH_2NO\ (I1) < HCNOH\ (I3, I3a, I3b) < CN(H)OH\ (I4) \leq HCN(H)O\ (I2, I2a)$$

where "a" and "b" represent higher energy conformations. All are planar (C_s symmetry) with $^2A'$ ground states (four electrons in a″ MO's). Interconversion is possible either by direct 1,2- or 1,3-hydrogen migration, or alternatively via an initial ring closure followed by a 1,2-hydrogen migration and by ring opening. It is interesting to note that only one conformation of CN(H)OH, viz. I4, where the two hydrogens are trans to each other, is a stable isomer. The cis conformer (TS7) was found to possess an imaginary a″ frequency and thus identified as the transition state associated with the barrier to rotation of the O-bound hydrogen around the N−O bond. There are only two

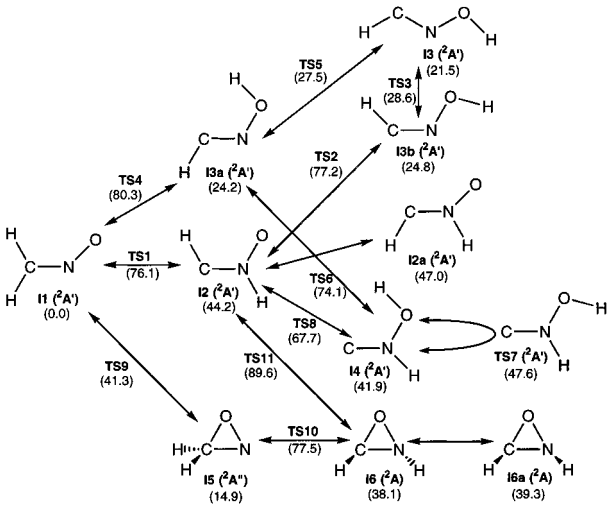

Figure 3. Reaction pathways for the interconversion of CNO-chain isomers of CH_2NO. (The G2 energies in parentheses are relative to CH_2NO in kcal/mol.)

stable cyclic isomers: cyclic $CH_2NO(^2A'')$ (I5), which in energy lies between I1 and I3, and cyclic C(H)N(H)O(^{2}A) (I6, I6a) which lie between I3b and I4. Formation of these from the parent molecule I1 may also proceed in either of two ways: ring closure, then hydrogen transfer, or hydrogen transfer, then ring closure. Figure 3 summarizes the possible pathways available for the various isomerizations. We now discuss each of these reaction pathways.

CH_2NO → HCN(H)O (I2, I2a) → HCNOH (I3b, I3)/I2 → CN(H)OH (I4). The computed schematic G2 PES for these reactions is shown in Figure 4 with the corresponding relative energies in Table 3. The lowest energy pathway for the production of HCN(H)O (I2) from CH_2NO proceeds by a 1,2-H migration and takes place entirely on the $^2A'$ surface via transition state TS1. The barrier height for this process is fairly high at 76.1 kcal/mol which may be attributed partly to the steric

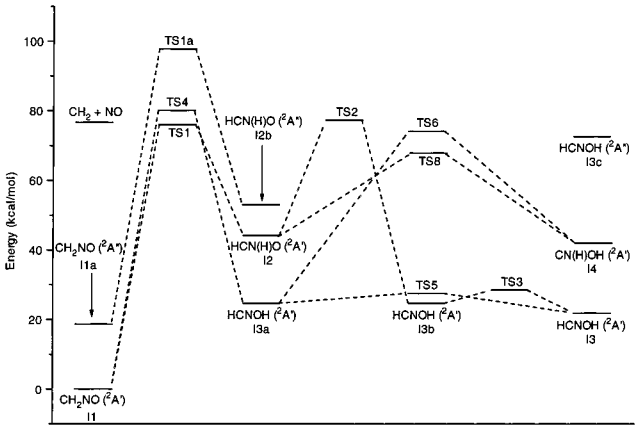

Figure 4. Schematic G2 potential energy surface for the interconversion of open CNO-chain isomers of CH_2NO. (The energies are relative to CH_2NO.)

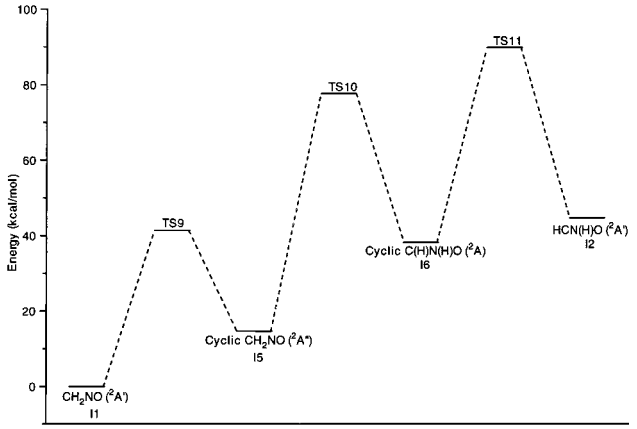

Figure 5. Schematic G2 potential energy surface for the interconversion of CNO-chain isomers of CH_2NO via ring structures. (The energies are relative to CH_2NO.)

TABLE 3: G2 Energies of Isomers and Transition States Associated with the Isomerization Reactions of CH_2NO (Relative to $CH_2NO(^2A')$, in kcal/mol)[a]

	G2		G2
$CH_2NO(^2A'')$ (I1a)	18.76[b]	HNC(H)O(^{2}A) (I7)	−19.99
TS1(^{2}A′)	76.13	HNC(H)O(^{2}A′) (I7a)	−11.75
TS1a(^{2}A″)	97.71[c]	HNC(H)O(^{2}A′) (I7b)	−9.32
HCN(H)O(^{2}A′) (I2)	44.16	SC13(^{2}A′/^{2}A″)	∼58.44[d]
HCN(H)O(^{2}A′) (I2a)	46.97	$NCH_2O(^2A')$ (I8)	56.80
HCN(H)O(^{2}A″) (I2b)	52.72	TS14(^{2}A)	55.88
TS2(^{2}A′)	77.24[d]	TS15(^{2}A)	9.73
HCNOH(^{2}A′) (I3b)	24.75	TS15a(^{2}A)	11.41
TS3(^{2}A′)	28.56[d]	$NH_2CO(^2A')$ (I9)	−41.05
HCNOH(^{2}A′) (I3)	21.52	$NH_2CO(^2A'')$ (I9a)	30.42
HCNOH(^{2}A″) (I3c)	72.30	TS16(^{2}A″)	−21.47[d]
TS4(^{2}A′)	80.27	TS16a(^{2}A″)	−19.22[d]
HCNOH(^{2}A′) (I3a)	24.23	TS16b(^{2}A′)	−9.57
TS5(^{2}A)	27.54	TS17(^{2}A′)	19.73
TS6(^{2}A)	74.11	HNCOH(^{2}A′) (I10a)	−20.58
CN(H)OH(^{2}A′) (I4)	41.91	TS18(^{2}A)	−16.04
TS7(^{2}A′)	47.61	HNCOH(^{2}A′) (I10)	−21.19
TS8(^{2}A′)	67.70	TS19(^{2}A′)	13.26
TS9(^{2}A)	41.30	TS20(^{2}A)	60.07
cyclic $CH_2NO(^2A'')$ (I5)	14.85	NC(H)OH(^{2}A′) (I11)	−23.93
TS10(^{2}A)	77.48	TS21(^{2}A)	−17.48
cyclic C(H)N(H)O(^{2}A) (I6)	38.06	NC(H)OH(^{2}A′) (I11a)	−20.88
cyclic C(H)N(H)O(^{2}A) (I6a)	39.25	TS22(^{2}A)	17.49
TS11(^{2}A)	89.59	TS23(^{2}A′)	11.68
TS12(^{2}A)	45.54	TS24(^{2}A)	18.21

[a] At MP2/6-31G(d) geometry. [b] Possesses an imaginary a″ frequency. [c] Second-order saddle point. [d] Using scaled MP2 frequencies.

strain of the three-membered H_2-C-N ring, which generates small HCN and HNC angles, but also to the extensive electronic reorganization that takes place. In CH_2NO the unpaired electron is located primarily on the oxygen whereas in TS1 and the product I2 it is located almost exclusively on the carbon (according to the MP2 spin densities). I2 is the lowest energy isomer of HCN(H)O with a relative energy of 44.2 kcal/mol, with the two hydrogens trans to each other. The corresponding planar cis isomer I2a (^{2}A′) lies slightly higher at 47.0 kcal/mol and may be easily formed by rotation around the CN bond. Further migration of the same hydrogen onto the oxygen proceeds via TS2 (which is ∼1 kcal/mol higher in energy than TS1) and results in a fairly stable isomer, viz. HCNOH, which can exist in one of three forms: I3, I3a, and I3b. These conformers easily interconvert, however, via low-energy transition states TS3 and TS5. The most stable of these is I3 with an energy that is just 21.5 kcal/mol higher than $CH_2NO(^2A')$. In addition to their A′ states, CH_2NO and HCN(H)O have low lying A″ excited states, as indicated in Figure 4. In the case of I2 the A″ state lies just 8.5 kcal/mol above the A′ state. However, the A″ transition state associated with the formation of this species from the A″ state of CH_2NO has a very high energy: ∼100 kcal/mol above the ground state of CH_2NO. Consequently, the isomerization reactions on the A″ surface were not investigated further.

Rather than undergoing a 1,2-H shift, I2 may also undergo a 1,3-H shift from carbon to oxygen to yield CN(H)OH (I4), via a relatively low energy transition state: TS8. Once again, this takes place on the ^{2}A′ surface. As noted above, I4 is the only stable conformation of CN(H)OH. An alternative route for its formation is from I3a, by a 1,2-H transfer via TS6, as indicated in Figures 3 and 4.

CH_2NO → HCNOH (I3a, I3)/I3a → CN(H)OH (I4). The schematic G2 potential surface for these reactions is also shown in Figure 4 with relative energies given in Table 3. Formaldiminoxy itself may undergo a 1,3-hydrogen migration reaction via TS4 to form HCNOH (I3a) on the ^{2}A′ surface. The energy of this transition state is 80.3 kcal/mol, considerably higher than the analogous barrier for the 1,3-shift via TS8 described above and actually lying ∼4 kcal/mol above the dissociation limit (to CH_2 and NO). The existence of this high-energy transition state is likely to be an artifact of the MP2 geometry optimization, especially since we were unable to locate it at the CASSCF level. Our attempts to find it using CASSCF resulted in a transition state corresponding to the association/dissociation of hydrogen to/from oxygen in I3a. Consequently, it is highly likely that the pathway to I3a is via I2 → I3b → I3 → I3a. As noted already, the interconversion among the HCNOH isomers is expected to be very facile.

The possibility also exists that HCNOH (I3a) can undergo a 1,2-H shift to yield CN(H)OH (I4). Both reactant and product are planar species with ^{2}A′ ground states, but the transition state associated with this H shift, viz. TS6, is nonplanar. As for TS4, no CASSCF transition state could be found corresponding to TS6. The CASSCF optimizations consistently produced a transition state for the association/dissociation of I3a from/to HCN + OH.

CH_2NO → Cyclic CH_2NO (I5) → Cyclic C(H)N(H)O (I6, I6a) → HCN(H)O (I2). As indicated in Figure 3, CH_2NO can cyclize and then isomerize. The G2 PES for these processes are summarized in Figure 5. As can be seen, these provide an alternative pathway for the formation of HCN(H)O (I2). The first step in this process is the low-barrier ring-closing reaction of CH_2NO to cyclic CH_2NO (I5) that was discussed in our

previous paper on CH_2NO. During this reaction, a change of symmetry occurs, as I5 has a $^2A''$ ground state, i.e., five electrons in a″ MO's in the SCF configuration. After CH_2NO (I1), this is the most stable isomer depicted in Figure 3.

Cyclic CH_2NO can now undergo a 1,2-H shift from carbon to nitrogen. The situation resembles the 1,2-H shifts involving the straight-chain isomers in that a "tight" three-membered H_2-C-N ring is formed in the transition state (TS10, energy 77.5 kcal/mol), which corresponds to a sizable barrier height of 62.6 kcal/mol. Complete severing of the H_2-C bond allows the formation of the H_2-N bond and produces the second ring isomer, namely, cyclic C(H)N(H)O (I6, 38.1 kcal/mol), in which the two hydrogens are positioned trans to each other. I6 is a chiral molecule and the enantiomer so formed depends on whether it is the hydrogen above or below the CNO plane in I5 that is being transferred. Of course, the two pathways are energetically equivalent, both occurring via TS10 (or its mirror image) to give I6 (or its mirror image). The cis isomer, I6a, is slightly higher in energy at 39.3 kcal/mol and it too exists as an enantiomeric pair, one enantiomer having both hydrogens above the plane, the other having both hydrogens below it.

From I6 a linear CNO chain, i.e., I2, can be regenerated by breaking the CO bond. As this occurs, the two hydrogens rotate in the same sense. (For I6 in Figure 2 this is anticlockwise when looking along the C−N bond from carbon to nitrogen.) The barrier height at TS11 (energy 89.6 kcal/mol) is 51.5 kcal/mol, slightly higher than for the original ring closure. Nevertheless, in an absolute sense this pathway for the production of I2 is significantly more energetic than the simple 1,2-H migration in CH_2NO.

Reaction Pathways for CNO-Chain and Ring Isomerizations. By referring to Figures 3, 4, and 5, the lowest energy pathway for the formation of the most stable conformer of each isomer, i.e., I2, I3, I4, I5, and I6, from CH_2NO (I1), may be determined. Production of I2 is expected to proceed by a direct 1,2-H shift, while the most obvious pathway to I3 is by two consecutive 1,2-migrations, i.e., via I2 and I3b. Similarly, the lowest energy pathway for formation of I4 is via I2 and TS8. As to the ring-isomers, I5 is expected to form in the one-step ring-closing reaction via TS9. These results demonstrate that the minimum energy pathways for all CNO-chain isomers from CH_2NO involve the 1,2-carbon-to-nitrogen hydrogen transfer (TS1) as the first step. The energy barrier of 76.1 kcal/mol for this process is also the highest point on the PES for these isomerizations.

The CASPT2/cc-pVTZ and QCISD(T)/cc-pVTZ relative energies computed for selected species at their CASSCF/cc-pVDZ geometries are listed in Table 4. In most cases these results agree well with the corresponding G2 energies in Table 3, the only two exceptions being TS8 and TS11. The energies of these two transition states were also computed at their G2, viz. MP2/6-31G(d), geometries and are also listed in Table 4. With regard to TS8, the MP2 and CASSCF geometries differ appreciably in the parameters specifying the position of the migrating hydrogen and this is reflected in the energetics. The G2, CASPT2, and QCI energies at the MP2 geometry are all comparable, but lower than the CASPT2 and QCI energies calculated at the CASSCF geometry. Since the CASSCF geometry should be more reliable for this transition state, these results suggest that the G2 estimate of the barrier height is too low by about 5−8 kcal/mol. TS11 is somewhat different in that even though the two geometries are essentially alike (an attribute reflected by the agreement of the energies in Table 4), its G2 energy is quite high, particularly in comparison with CASPT2. It would seem that in this case G2 does a good job at finding the geometry but is unable to account accurately for the correlation energy, overestimating the barrier by 3−8 kcal/mol as a result. As noted already, in the case of TS4 and TS6, no corresponding transition states were found at the CASSCF level. Thus, rather than by a direct 1,3-H shift, HCNOH (I3a) would be expected to form via I2 or by dissociation to H + HCNO followed by recombination. Likewise, the nonexistence of TS6 suggests that the interconversion between I3a and CN(H)OH (I4) could occur via I2 as intermediate or by a dissociation/recombination reaction via H + HONC. These bimolecular mechanisms are discussed in our next paper.[23]

TABLE 4: CASPT2 and QCISD(T) Energies (Including Zero-Point Correction) of Selected Isomers and Transition States Associated with the Isomerization Reactions of CH_2NO (Relative to $CH_2NO(^2A')$, in kcal/mol)[a]

	CASPT2(11/11) cc-pVTZ	QCISD(T) cc-pVTZ
TS1($^2A'$)	78.9	74.6
TS2($^2A'$)	80.5	79.2
TS8($^2A'$)	76.1	71.5
	67.5[b]	66.9[b]
TS9(^2A)	41.4	42.6
CN(H)OH($^2A'$) (I4)	46.1	40.7
cyclic $CH_2NO(^2A'')$ (I5)	17.5	14.5
TS10(^2A)	79.5	77.1
TS11(^2A)	81.4	84.6
	82.5[b]	86.8[b]
TS12(^2A)	45.5	42.1

[a] At CASSCF(11/11)/cc-pVDZ geometry unless stated otherwise. [b] At MP2/6-31G(d) geometry.

Overall, both MP2 and CASSCF methods give rise to very similar geometries and energies. When this is not the case, as found for certain transition states, there does not seem to be an obvious reason for the discrepancies. For example, the three energies for TS9 all agree very closely whereas for TS11, which is also a ring-opening, C−O bond-breaking reaction, the range of energies spanned is much larger. Furthermore, it is not obvious why no CASSCF geometry was found for TS6, since, first, transition states for the other three 1,2-H shifts *are* found at this level and, second, there seem to be no unusual features to TS6 when studied by MP2.

The revised energies for TS8 and TS11 do not greatly alter the conclusions reached on the basis of G2 energies concerning the lowest energy CNO-chain and ring isomerization pathways. TS1 is predicted to be the highest point on the potential energy surface for all CNO-chain isomerizations, irrespective of theory and/or the choice of energy for TS8. Also, as the revised energy for TS11 is now lower than before, the formation of I2 via the channel involving the cyclic structures is more favorable than found previously. Therefore, production of I6 via I2 is now also more likely, although the channel via I5 is expected to remain the lowest energy pathway.

NCO-Chain Isomers. The cyclic isomers I5 and I6 could ring open by NO bond rupture, resulting in open chain isomers with a NCO backbone. These then have the capacity to undergo a variety of H transfer reactions. The MP2/6-31G(d) and CASSCF(11/11)/cc-pVDZ geometries of the various isomers and transition states with the NCO structure are summarized in Figures 6, 7 and 8. The associated G2, CASPT2 and QCISD-(T) energies are listed in Tables 1 and 2. Five stable isomers were found on the molecular potential energy surface. In order of energy these are

NH_2CO (I9) < NC(H)OH (I11) ≤ HNCOH (I10) ≤ HNC(H)O (I7) ≪ NCH_2O (I8)

With the exception of I8, all the above isomers are more stable than the most stable CNO-chain isomer, viz. CH_2NO (I1). I8 is a nitrene; i.e., the nitrogen has two lone pairs of electrons, and thus both the CN and CO bonds are just σ-bonds. Not surprisingly, the CN bond is in fact the longest among all the isomers studied in this work. As for the CNO-chain isomers, each NCO type isomer possesses C_s symmetry and a $^2A'$ ground state with the exception of I7 which is nonplanar. The planar conformations of I7 have $^2A''$ ground states but they are transition states connecting the two enantiomers of I7. The various pathways by which the isomerization reactions of these molecules could occur are summarized in Figure 9. Each of these will now be discussed.

Cyclic C(H)N(H)O (I6) → HNC(H)O (I7, I7a, I7b) → NCH_2O (I8) → Cyclic CH_2NO (I5). The schematic G2 PES for these reactions is shown in Figure 10. I7 can form directly from I6 (which can itself be formed from I5) by a simple one-step ring-opening reaction via a low-energy transition state (TS12 with energy 45.5 kcal/mol above CH_2NO). The actual barrier to this reaction is only 7.5 kcal/mol, which is considerably lower than the analogous barrier to ring opening in the CNO chain system (TS11). Furthermore, the product I7 is much more stable than the analogous CNO product, viz. I2. I7 is chiral, in analogy with the other species with C_1 symmetry, viz. I6 and I6a, and as to which enantiomer is formed depends on the choice of its precursor, I6. The two forms of I7 can easily interconvert via a planar transition state in which the N-bound hydrogen is either cis (TS16) or trans (TS16a) to the oxygen. The G2 energy of I7 is actually above that of TS16, although of course at the MP2 level (that is used to determine the G2 geometries), both TS16 and TS16a are saddle points on the PES and have higher energies than I7 (by 5.2 and 9.8 kcal/mol, respectively). The imaginary frequency in each is associated with a torsional normal mode of a″ symmetry. It is nevertheless possible that at a higher level of theory I7 would be predicted to be planar and a nonplanar geometry would correspond to a transition state. This is an example of the contradiction that can result when a composite method such as G2 is used to characterize closely lying stationary points on the PES. The lowest cis and trans electronic excited states of I7 (I7a and I7b) are planar, of A′ symmetry, and lie 8.2 and 10.7 kcal/mol above I7, as predicted by G2. These states thus correlate with the ground ($^2A'$) states of the other planar isomers.

I7 can also form in a two-step process from I5 via I8. The first step is ring opening, to produce I8. Since the reactant and product have different electronic symmetries, (diabatic) curve crossing needs to be invoked, whereby the system crosses from the $^2A''$ to the $^2A'$ surface. This can occur by vibronic coupling. At the equilibrium geometry of I5 ($^2A''$) the separation between the ground and first excited ($^2A'$) state is quite high but as the reaction proceeds and the NCO angle opens up this separation steadily decreases. The crossover point occurs when the NCO angle becomes ∼102° (SC13) where the energy is ∼58.4 kcal/mol above I1. Along the $^2A''$ surface the energy rapidly increases with the reaction coordinate, but there is only a slight decrease in the energy of the $^2A'$ state since the crossover point occurs very near the equilibrium geometry of I8 ($^2A'$) where the NCO angle is ∼115.0°. Thus, the reverse barrier height is only 1.6 kcal/mol so that I8 is formed at a relatively high energy of 56.8 kcal/mol that stems from its unusual nitrenic electronic structure, as indicated above.

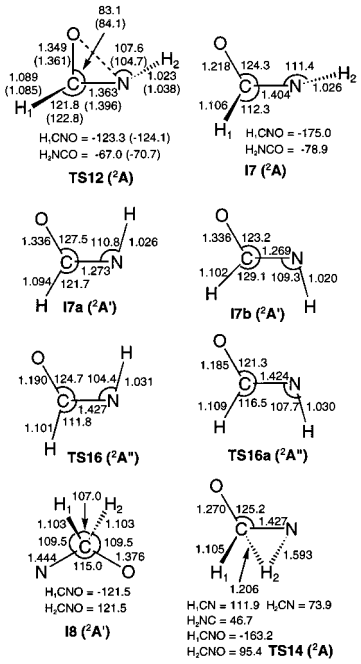

Figure 6. MP2/6-31G(d) geometries and CASSCF(11/11)/cc-pVDZ geometries (in parentheses) of species corresponding to stationary points on the PES describing the NCO chain isomerizations (in Å and deg).

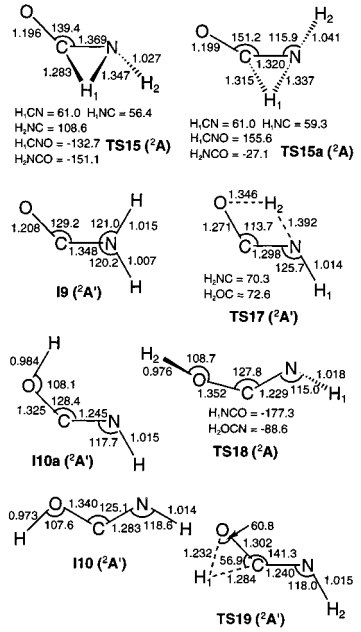

Figure 7. MP2/6-31G(d) geometries of species corresponding to stationary points on the PES describing the NCO chain isomerizations (in Å and deg).

I8 is clearly a metastable molecule, as it can readily isomerize to I7 by a 1,2-H shift, from carbon to nitrogen, breaking the C_s symmetry in the process. Again, the G2 energy for the transition state (TS14 with energy 55.9 kcal/mol above CH_2NO) is slightly lower than that for I8, although at the MP2 level the corresponding (forward) barrier height is 16.3 kcal/mol and TS14 is a true saddle point connecting I7 and I8. Nevertheless, it is possible that at a higher level of theory I8 would not be predicted to be a (meta-) stable intermediate. As to which enantiomer of I7 forms, depends on which of the two hydrogens migrates.

HNC(H)O (I7) → NH_2CO (I9) → HNCOH (I10a, I10). The PES of these H-transfer reactions is summarized in Figure 11. The first of these 1,2-H shifts results in NH_2CO (I9), which

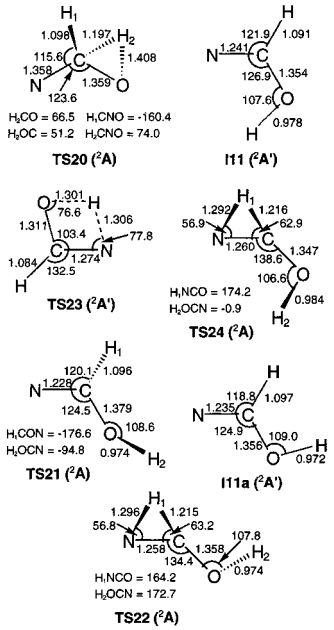

Figure 8. MP2/6-31G(d) geometries and CASSCF(11/11)/cc-pVDZ geometries (in parentheses) of species corresponding to stationary points on the PES describing the NCO chain isomerizations (in Å and deg).

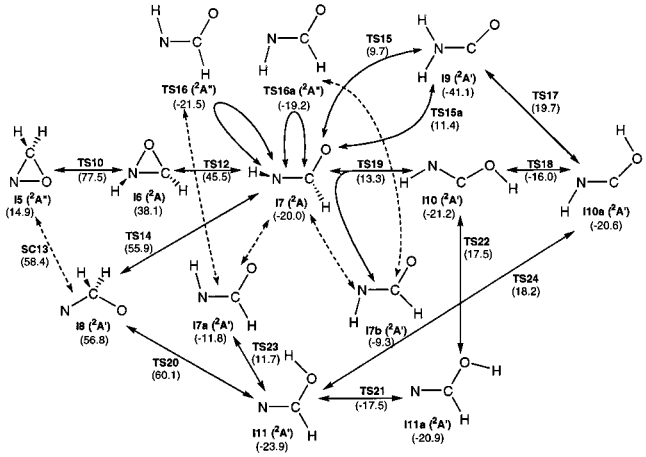

Figure 9. Reaction pathways for the interconversion of NCO-chain isomers of CH_2NO. Dashed lines represent transitions between the A′ and A″ surfaces. (The G2 energies in parentheses are relative to CH_2NO in kcal/mol.)

is by far the most stable isomer of the formaldiminoxy system. There are two distinct transition states associated with the isomerization of nonplanar I7 to I9, TS15 and TS15a, which correspond to the two hydrogens being on opposite or the same sides of the NCO plane, respectively. The energies are very similar and, of course, the only way to possibly distinguish between the two mechanisms is by isotopic substitution. No transition states were found, at the MP2 level at least, for the analogous H-transfer in the planar $^2A'$ states of I7a or I7b. The attempts to locate these resulted in a transition state for the dissociation reaction to H + HNCO (with very long H−N and H−C distances).

Once NH_2CO (I9) has formed, a 1,3-H transfer (from nitrogen to oxygen) leads to HNCOH. This reaction takes place entirely on the $^2A'$ surface with a fairly high barrier corresponding to TS17, but which is still only 19.7 kcal/mol above CH_2NO. Initially HNCOH is in the higher energy conformation (I10a with an energy of 20.6 kcal/mol below CH_2NO). The transformation to the lower energy conformation I10 ($^2A'$) occurs by

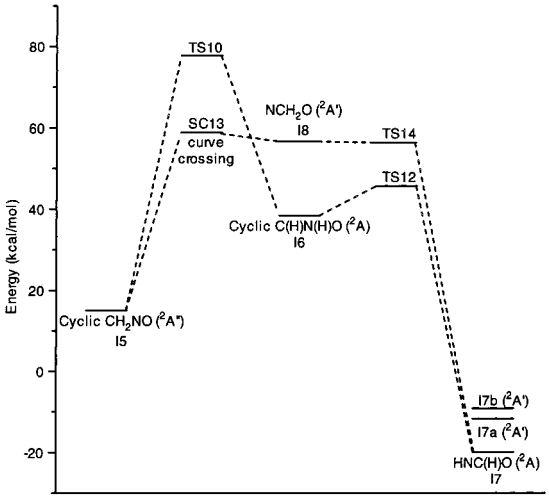

Figure 10. Schematic G2 potential energy surface for the interconversion of NCO-chain isomers of CH_2NO. (The energies are relative to CH_2NO.)

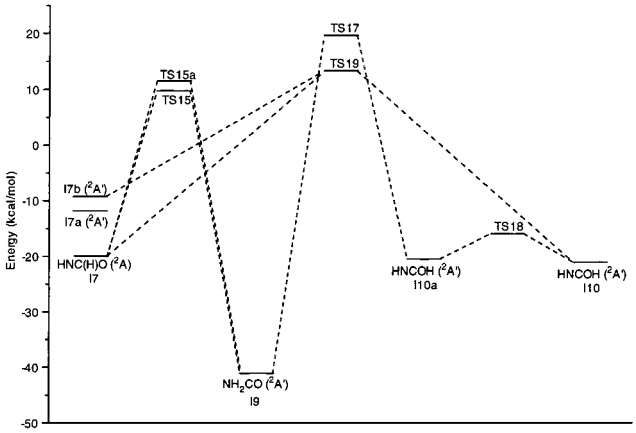

Figure 11. Schematic G2 potential energy surface for the interconversion of open NCO-chain isomers of CH_2NO. (The energies are relative to CH_2NO.)

rotation around the O−C bond, with a barrier of just 4.5 kcal/mol.

I10 may also be produced from I7 by a 1,2-H shift and this reaction gives rise to some interesting features. We find that as the transition state TS19 is approached the molecule gradually becomes planar, but the electronic state is now $^2A'$, rather than $^2A''$ as in TS16 and TS16a. Note that in the process the N-bound hydrogen (H_2) places itself trans to the oxygen. In the transition state the other hydrogen (H_1) is part of a tight three-membered ring, similar to the transition states for the other 1,2-H shifts discussed earlier. The critical energy of this reaction is just 33.3 kcal/mol. The formation of I10 from I7b, noting that both are in $^2A'$ states, occurs via the same transition state (TS19) as the reaction discussed above. The I7 to I7b transition might be accomplished by electronic excitation followed by vibrational relaxation to the planar geometry, or even thermally, given the small energy gap.

Considering the reverse process, i.e., migration of hydrogen from oxygen to carbon in I10, it is clear that at some point on the PES, once the transition state is passed, there is a bifurcation or branching on the PES. Thus, if planarity is maintained, I7b will be the product, but if the system breaks symmetry, it will end up as I7.

NCH_2O (I8) → NC(H)OH (I11, I11a) → HNC(H)O (I7a, I7)/HNCOH (I10a, I10). The schematic G2 potential energy

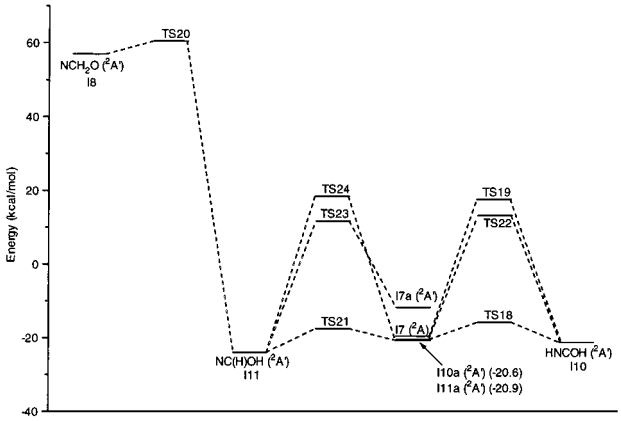

Figure 12. Schematic G2 potential energy surface for the interconversion of open NCO-chain isomers of CH_2NO. (The energies are relative to CH_2NO.)

surfaces for these reactions are depicted in Figure 12. The isomerization of NCH_2O (I8) to NC(H)OH (I11) occurs by a simple 1,2-H shift from carbon to oxygen. As H_2 migrates toward oxygen it also twists around the C−O bond (anticlockwise when viewed from carbon to oxygen) so that in the transition state (TS20) the H_2−C−O triangle is near-perpendicular to the N−C−O triangle. The energy at this point, 60.1 kcal/mol (relative to CH_2NO), corresponds to a (forward) barrier height of only 3.3 kcal/mol and suggests that I8 will isomerize to NC(H)OH (via TS20) or to HNC(H)O (via TS14) with equal ease (assuming that the Arrhenius *A* factors are also comparable). In TS20 the atom "H_2" is oriented such that it could form either of the two NC(H)OH conformers I11 and I11a in which the O-bound hydrogen is cis or trans to nitrogen. However, following the reaction coordinate leads to the cis equilibrium structure I11 ($^2A'$). This has an energy of −23.9 kcal/mol (relative to CH_2NO) and lies ∼3 kcal/mol lower in energy than the trans isomer I11a. The two isomers can readily interconvert however, via TS21.

I11 can readily isomerize to I7a and hence to I7, by a 1,3-H shift, via TS23. In line with the other 1,3-shifts encountered previously, the reaction maintains planarity, i.e., it occurs on the $^2A'$ surface. The barrier is quite low at 35.6 kcal/mol, considerably lower for example than the barrier for the 1,3-H shift in I9 resulting in I10a, viz. 60.8 kcal/mol.

I11 may also undergo a 1,2-H shift from carbon to nitrogen to yield I10a, which takes place via TS24, which also represents a low energy barrier. Although both reactant and product are planar with $^2A'$ ground states, TS24 is actually slightly nonplanar. The H transfer process is qualitatively similar to the 1,2-shift between I3a and I4 (via TS6) discussed earlier but the geometry of TS6 is highly nonplanar. The critical energy of the I11 → I10a reaction is 42.1 kcal/mol, which is comparable with that for the I3a → I4 reaction, viz. 50.1 kcal/mol, but again, in absolute terms, the energetics for these NCO reactions are much lower than for the CNO systems. The interconversion of I10a and I10 via TS18 is a very facile reaction, as discussed already.

An alternative route between I11 and I10 is to effect the 1,2-H shift after the desired trans conformation has been achieved, i.e., utilizing I11a as an intermediate. The first step, where the higher energy conformer of NC(H)OH, I11a ($^2A'$, energy −20.9 kcal/mol) is generated, occurs by rotation of the O-bound hydrogen around the O−C bond, via the transition state TS21. The critical energy of this process is only 6.5 kcal/mol. I11a can then directly isomerize to I10 by a 1,2-H shift from carbon to nitrogen via a nonplanar transition state (TS22, energy 17.5 kcal/mol) whose structure is quite similar to TS24. The barrier associated with the hydrogen transfer is 38.4 kcal/mol. The difference in the overall barrier heights of the two pathways connecting I10 and I11 is only 0.7 kcal/mol, indicating that on energetic grounds the two processes may be expected to have similar rate constants.

TABLE 5: G2 Heats of Reactions and the Resulting Heats of Formation of CH_2NO (I1) and NH_2CO (I9) (in kcal/mol)

reaction	$\Delta_r H^\circ_{298}$	$\Delta_f H^\circ_{298}$-(CH_2NO)	$\Delta_f H^\circ_{298}$-(NH_2CO)
$CH_2(^3B_1) + NO \rightarrow CH_2NO$ (1)	−78.2	35.8	
$CH_2NO + NO_2 + CH_4 \rightarrow$ $CH_3NO + NO + CH_3$ (2)	9.5	37.5	
$CH_2NO \rightarrow NH_2CO$ (3)	−40.8		−3.3[a]
$NH_2CO + CH_4 \rightarrow CH_3NO + NH_3$ (4)	7.7		−3.6
$NH_2CO + CH_3CH_3 \rightarrow$ $NH_2C(CH_3)O + CH_3$ (5)	7.8		−4.0

[a] Using $\Delta_f H^\circ_{298}$ (CH_2NO) = 37.5 (kcal/mol).

Reaction Pathways for NCO-Chain Isomerizations. The various isomerization schemes are depicted in Figure 9. The formation of NCO-chain isomers from CH_2NO must proceed via one of the cyclic intermediates I5 or I6. On energetic grounds the most favorable mechanism is the cyclization of CH_2NO to I5, followed by ring-opening to I8. The highest barrier encountered on this pathway occurs in the form of curve crossing in the ring-opening step, computed to be 58.4 kcal/mol. Of the two options available to I8 for further isomerization, the 1,2-shift to yield I7 is associated with the lower barrier, with a height of 55.9 kcal/mol. All other NCO-chain species can be generated from I7 by low-energy isomerizations. Thus, the rate-determining step for the formation of all NCO-chain isomers is expected to be the curve crossing that results in I8. We note also that cyclic C(H)N(H)O (I6) can also be produced in the same manner (and with the same barriers) as the NCO chains via I7, and overall this represents a significantly more favorable pathway energetically, by about 19 kcal/mol, than the direct 1,2-H shift from I5.

Heats of Formation of CH_2NO and NH_2CO. The heats of formation, $\Delta_f H^\circ_{298}$, of CH_2NO (I1) and NH_2CO (I9) were calculated from the computed G2 heats of reactions, $\Delta_r H^\circ_{298}$, of a series of hypothetical reactions involving I1 and I9 and experimental heats of formation[29−33] of all other species in the reactions. The results are summarized in Table 5. With the exception of (1), all the reactions are isogyric, with (5) being actually isodesmic. The computed heats of formation are remarkably consistent, especially if reaction 1 is disregarded. It has been noted by Sendt et al.,[34] in the context of singlet/triplet separations in several carbenes, that G2 has a tendency to underestimate the stability of triplet states by ∼2.4 kcal/mol. Applying such a correction to the computed heat of reaction of (1) would result in the heat of formation of CH_2NO being 2.4 kcal/mol higher, viz. 38.2 kcal/mol, which then, using reaction 3, would result in a heat of formation of −4.0 kcal/mol for NH_2-CO. Given the overall consistency of these results but also the existence of experimental errors in the thermochemical data used, our conservative estimates of the heats of formation of CH_2NO and NH_2CO are 37.5 ± 1 and −3.6 ± 1 kcal/mol, respectively.

Conclusion

The study of the potential energy surfaces associated with the unimolecular isomerization reactions of formaldiminoxy has demonstrated that while there are numerous pathways by which

a given isomer can be formed, most low-energy pathways have one or more common intermediates. Open-chain isomers containing CNO-chain backbones are generally more energetic than their NCO-chain counterparts and their isomerization reactions access transition states whose energies are also significantly higher in most instances than those of the NCO-chain rearrangements. Consequently, with respect to the decomposition of formaldiminoxy, the NCO-chain isomers are expected to play an important role, depending of course on the mechanisms of decomposition of the individual isomers, which is the topic of part 2 of this study.[23] The gateway to the formation of NCO-chain isomers is the cyclic isomer of CH_2-NO (I5) that yields the open-chain isomer NCH_2O which in turn can further isomerize to yield all other NCO-chain isomers. The lowest energy isomers of formaldiminoxy are NH_2CO, NC(H)OH, HNCOH, and HNC(H)O with energies of 41.1, 23.9, 20.6, and 20.0 kcal/mol below that of CH_2NO.

Acknowledgment. The award of a Sydney University Postgraduate Scholarship to W.A.S. is gratefully acknowledged.

References and Notes

(1) Miller, J. A.; Bowman, C. T. *Prog. Energy Combust. Sci.* **1989**, *15*, 287 and references therein.

(2) Fenimore, C. P. In *13th Symposium (International) on Combustion*; The Combustion Institute: Pittsburgh, PA, 1971; p 373.

(3) Wendt, J. O. L.; Sternling, C. V.; Matovich, M. A. In *14th Symposium (International) on Combustion*; The Combustion Institute: Pittsburgh, PA, 1973; p 897.

(4) Myerson, A. L. In *15th Symposium (International) on Combustion*; The Combustion Institute: Pittsburgh, PA, 1975; p 1085.

(5) Song, Y. H.; Blair, D. W.; Siminski, V. J.; Bartok, W. In *18th Symposium (International) on Combustion*; The Combustion Institute: Pittsburgh, PA, 1981; p 53.

(6) Chen, S. L.; McCarthy, J. M.; Clark, W. D.; Heap, M. P.; Seeker, W. R.; Pershing, D. W. In *21st Symposium (International) on Combustion*; The Combustion Institute: Pittsburgh, PA, 1986; p 1159.

(7) Laufer, A. H.; Bass, A. M. *J. Phys. Chem.* **1974**, *78*, 1344.

(8) Vinckier, C.; Debruyn, W. *J. Phys. Chem.* **1979**, *83*, 2057.

(9) Seidler, V.; Temps, F.; Wagner, H. Gg.; Wolf, M. *J. Phys. Chem.* **1989**, *93*, 1070.

(10) Atakan, B.; Kocis, D.; Wolfrum, J.; Nelson, P. In *24th Symposium (International) on Combustion*; The Combustion Institute: Pittsburgh, PA, 1992; p 691.

(11) Cyr, D. R.; Leahy, D. J.; Osborn, D. L.; Continetti, R. E.; Neumark, D. M. *J. Chem. Phys.* **1993**, *99*, 8751.

(12) Farmer, J. B.; Gardner, C. L.; Gerry, M. C. L.; McDowell, C. A.; Raghunathan, P. *J. Phys. Chem.* **1971**, *75*, 2448.

(13) McCluskey, M.; Frei, H. *J. Phys. Chem.* **1993**, *97*, 5204.

(14) Shapley, W. A.; Bacskay, G. B. *Theor. Chem. Acc.* **1998**, *100*, 212.

(15) Curtiss, L.; Raghavachari, K.; Trucks, G.; Pople, J. *J. Chem. Phys.* **1991**, *94*, 7221.

(16) Roos, B. O.; Taylor, P. R.; Siegbahn, P. E. S. *Chem. Phys.* **1980**, *48*, 157.

(17) Roos, B. O. In *Ab Initio Methods in Quantum Chemistry-II*.; Lawley, K. P., Ed.; J. Wiley & Sons Ltd.: Chichester, UK, 1987; p 399.

(18) Pople, J. A.; Head-Gordon, M.; Raghavachari, K. *J. Chem. Phys.* **1987**, *87*, 5968.

(19) Watts, J. D.; Gauss, J.; Bartlett, R. J. *J. Chem. Phys.* **1993**, *98*, 8718.

(20) Andersson, K.; Malmqvist, P.; Roos, B. O.; Sadlej, A. J.; Wolinski, K. *J. Phys. Chem.* **1990**, *94*, 5483.

(21) Andersson, K.; Malmqvist, P.; Roos, B. O. *J. Chem. Phys.* **1992**, *96*, 1218.

(22) Roggenbuck, J.; Temps, F. *Chem. Phys. Lett.* **1998**, *285*, 422.

(23) Shapley, W. A.; Bacskay, G. B. *J. Phys. Chem. A* **1999**, *103*, 4514.

(24) Dunning, T. H. *J. Chem. Phys.* **1989**, *90*, 1007.

(25) Bacskay, G. B.; Martoprawiro, M.; Mackie, J. C. *Chem. Phys. Lett.* **1998**, *290*, 391.

(26) Frisch, M. J.; Trucks, G. W.; Schlegel, H. B.; Gill, P. M. W.; Johnson, B. G.; Robb, M. A.; Cheeseman, J. R.; Keith, T.; Petersson, G. A.; Montgomery, J. A.; Raghavachari, K.; Al-Laham, M. A.; Zakrzewski, V. G.; Ortiz, J. V.; Foresman, J. B.; Peng, C. Y.; Ayala, P. Y.; Chen, W.; Wong, M. W.; Andres, J. L.; Replogle, E. S.; Gomperts, R.; Martin, R. L.; Fox, D. J.; Binkley, J. S.; Defrees, D. J.; Baker, J.; Stewart, J. P.; Head-Gordon, M.; Gonzalez, C. and Pople, J. A. *Gaussian 94* (Revision B.3); Gaussian, Inc.: Pittsburgh, PA, 1995.

(27) Helgaker, T.; Jensen, H. J. Aa.; Jørgensen, P.; Olsen, J.; Ruud, K.; Ågren, H.; Andersen, T.; Bak, K. L.; Bakken, V.; Christiansen, O.; Dahle, P.; Dalskov, E. K.; Enevoldsen, T.; Fernandez, B.; Heiberg, H.; Hettema, H.; Jonsson, D.; Kirpekar, S.; Kobayashi, R.; Koch, H.; Mikkelsen, K. V.; Norman, P.; Packer, M. J.; Saue, T.; Taylor, P. R.; Vahtras, O. *DALTON, an ab initio electronic structure program* (Release 1.0); 1997.

(28) Andersson, K.; Blomberg, M. R. A.; Fischer, M. P.; Karlström, G.; Lindh, R.; Malmqvist, P.; Neogrády, P.; Olsen, J.; Roos, B. O.; Sadlej, A. J.; Schütz, M.; Seijo, L.; Serrano-Andrés, L.; Siegbahn, P. E. M.; Widmark, P.-O. *MOLCAS* (Version 4); Lund University: Sweden, 1997.

(29) Chase, M. W., Jr. *J. Phys. Chem. Ref. Data* 1998, monograph 9, 1.

(30) Knobel, Y. K.; Miroshnichenko, E. A.; Lebedev, Y. A. *Bull. Acad. Sci. USSR, Div. Chem. Sci.* 1971, 425.

(31) Tsang, W. In *Energetics of Organic Free Radicals*; Martinho Simoes, J. A., Greenberg, A., Liebman, J. F., Eds.; Blackie Academic and Professional: London, 1996; p 22.

(32) Pittam, D. A.; Pilcher, G. *J. Chem. Soc., Faraday Trans. 1* **1972**, *68*, 2224.

(33) Barnes, D. S.; Pilcher, G. *J. Chem. Thermodyn.* **1975**, *7*, 377.

(34) Sendt, K.; Ikeda, E.; Bacskay, G. B.; Mackie, J. C. *J. Phys. Chem. A* **1999**, *103*, 1054.